Materials Research Bulletin 76 (2016) 365–369

Contents lists available at ScienceDirect

Materials Research Bulletin

journal homepage: www.elsevier.com/locate/matresbu

# Dense nanocrystalline yttrium iron garnet films formed at room temperature by aerosol deposition

Scooter D. Johnson *, Evan R. Glaser, Shu-Fan Cheng, Jennifer Hite

*U.S. Naval Research Laboratory, 4555 Overlook Ave., S.W. Washington, DC, 20375, United States*

ARTICLE INFO

*Article history:*
Received 31 July 2015
Received in revised form 30 November 2015
Accepted 15 December 2015
Available online 23 December 2015

*Keywords:*
A. Ceramics
A. Magnetic materials
A. Nanostructures
B. Microstructure
B. Magnetic properties

ABSTRACT

We have employed aerosol deposition to form polycrystalline yttrium iron garnet (YIG) films on sapphire at room temperature that are 90–96% dense. We characterize the structural and dynamic magnetic properties of the dense films using scanning electron microscopy, X-ray diffraction, and ferromagnetic resonance techniques. We find that the as-deposited films are pure single-phase YIG formed of compact polycrystallites ~20 nm in size. The ferromagnetic resonance mode occurs at 2829 G with a linewidth of 308 G. We perform a series of successive anneals up to 1000 °C on a film to explore heat treatment on the ferromagnetic resonance linewidth. We find the narrowest linewidth of 98 G occurs after a 750 °C anneal.

Published by Elsevier Ltd.

## 1. Introduction

Aerosol deposition (AD) is a thick-film deposition process that can produce hundreds-of-micrometers-thick films at a deposition rate of several micrometers per minute with resulting densities greater than 95% of the bulk. AD is typically performed at pressures less than 20 Torr in the deposition chamber [1]. The process shows the potential to scale up to very large deposition areas, and it can deposit conformally [2]. One of the most notable advantage of the AD process is that deposition takes place entirely at room temperature; without the need to heat the precursor material or the substrate. This enables formation of films with materials of dissimilar melting temperatures [3–5]. There have been many material systems studied by AD for a wide variety of uses such as inductors [6], abrasion-resistant coatings [7], piezoelectrics [8], multiferroics [9], magnetoelectrics [10] thermistors [11], thermoelectric films [12], flexible dielectrics [13], hard tissue implants and bioceramics [14], solid electrolytes [15], and photocatalysts [16]. The low-cost operation, high deposition rate, and simplicity of AD has spurred interest by researchers in Germany, France, Japan, Korea, and in the United States.

For many microwave devices, magnetic films of several hundreds of micrometers thick are required and would ideally be integrated directly into the circuit board elements. One challenge to realizing this integration is the high-temperature regime needed for fabricating ferrite films (see review by Harris et al. [17]). One example is in device miniaturization for RF circuits by reducing the footprint of the embedded inductors. The inductor size can be reduced by replacing the air-core with a magnetic material [18]. This is accomplished by fabricating inductors on top of a single-plane or sandwiched between a double-plane of a material such as Ni-Fe, Co-Zr-Ta, Co-Nb-Zr, or Co-Hf-Ta-Pd. These materials are chosen for their high permeability and low-melting temperature, which enables integration into a system-on-chip process by magnetron sputtering [19–22]. However, the low resistivity of these materials requires additional fabrication steps to decrease eddy current loss and to insulate the plane from the conductor. The solution is to deposit an oxide or polyimide layer between the conductor and plane [21] and/or fabricate slotted planes [20]. There have also been efforts to utilize higher resistivity magnetic materials fabricated with a copper inductor deposited directly onto the magnetic plane. Some examples [23–25] are $Y_{2.8}Bi_{0.2}Fe_5O_{12}$, $Ni_{0.4}Zn_{0.4}Cu_{0.2}Fe_2O_4$, $Co_7ZrO_9$, $(YLa)_3Fe_5O_{12}$, and $Y_3Fe_5O_{12}$ (YIG). While the processing steps are reduced by eliminating the need for an insulating layer, the high melting temperatures involved in the oxide deposition pose difficulty for incorporation into system-on-chip technology.

For this reason, AD appears to be a natural choice for realizing potential new advancements in magnetic integrated circuit technology. We have recently reported on the structural and magnetic properties of a 39 μm-thick film of YIG deposited by AD [26] with a density of ~50% of the theoretical bulk (5.17 g/cm$^3$ for

* Corresponding author.
*E-mail address:* scooter.johnson@nrl.navy.mil (S.D. Johnson).

http://dx.doi.org/10.1016/j.materresbull.2015.12.024
0025-5408/Published by Elsevier Ltd.

YIG). We then applied this AD coating process to fill a single-turn inductor which demonstrated a marked improvement to the inductor performance [6]. Additional work to improve the magnetic properties of the film by reducing the ferromagnetic resonance (FMR) linewidth and producing a more dense film could potentially further improve the inductance properties of the structure. For magnetic characterization we analyze the FMR linewidth spectra to gain insight into the magnetic properties of the film such as magnetic saturation, magnetic anisotropy, magnetic homogeneity, magnetic porosity, and compositional purity. Herein, we report on the continuation of developing AD for producing films with improved structural and magnetic properties for integration into magnetic circuit applications.

## 2. Experimental

Film formation by AD takes place in the deposition chamber which contains a substrate mounted to translational motors. The substrate is rastered across a particle ejection path formed by the spray nozzle. On the inlet side of the spray nozzle is the aerosol chamber that contains an aerosol of dry particles. The deposition process is achieved by creating a pressure difference between the aerosol chamber and the deposition chamber, which accelerates the particles to a velocity of several hundred meters per second. This is done by pumping on the deposition chamber while flowing gas into the aerosol chamber. Additional details on the operating principles and system design of AD have been reported previously [26].

For this study a YIG powder (*Trans-Tech Inc.*, Adamstown, MD) with an average individual particle size of 0.5 μm was prepared for deposition by sieving out agglomerates of diameter greater than 53 μm. The sieved powder was then placed in a Paragon KM14 ceramic furnace and dried a minimum of 24 h in purified air. The dried and sieved powder was then placed into the aerosol chamber fitted with 53 μm and 20 μm filters (not employed in our earlier work) in series with the spray nozzle. The parameters for all the depositions reported in this work are: 500 Torr pressure difference, 7.5 mm nozzle-substrate distance, 0.65 mm/s sweep rate, and nitrogen carrier gas (99.999% minimum purity). The deposition substrates were *a*-plane sapphire wafer chips 335 μm in thickness. Multiple samples were fabricated simultaneously for different characterization needs.

The film thickness profile and roughness were measured using a KLA Tencor Alpha-Step 500 profilometer with a stylus force of 7.6 mg. The horizontal scanning resolution was 1 μm and the vertical scanning resolution was 1 Å. Film mass was determined using a Sartorius M2P microbalance with 1 μg readability. The bulk density was estimated using the film and substrate mass, sapphire density (3.98 g/cm$^3$), and average film and substrate thickness. The sample was cross-sectioned and imaged using an FEI Nova 600 NanoLab system with focus ion beam (FIB) milling and SEM capability. Images of the cross-sections created via FIB milling were taken at a 52° tilt. The sectioned samples were analyzed for porosity using ImageJ image processing and analysis software. Top-surface images were taken using a Leo Supra 55 SEM using the InLens setting at 2 kV acceleration voltage, 6.3 mm working distance, and 30 μm aperture size. FMR measurements were carried out at room temperature in a commercial (E-300) Bruker 9.5 GHz spectrometer. Low microwave powers (0.5 mW) and modulation amplitudes (0.1 Oe) were employed to avoid saturation effects and possible distortion of the FMR lineshapes, respectively. The films were annealed in a Paragon KM14 ceramic furnace in air for 6–8 h. Crystallographic data were collected using a PANalytical X'pert XRD system. The x-ray source was a sealed tube emitting Cu $K_\alpha$ radiation in a line focus geometry at an operating voltage of 45 kV with a 40 mA current. The scan was performed with a 0.01° step size at 10 s/step.

## 3. Results

Fig. 1 shows top surface and cross-sectional images of an as-deposited film. In Fig. 1(a) and (b) the top surface of a representative as-deposited film is shown at two magnifications. Fig. 1(a) reveals a lower magnification broad view of the film structure. As evident in the image, much of the film is comprised of dense and compact material with individual particles much smaller than the individual starting particles of 0.5 μm. Fig. 1(b) is a magnified image of the film surface. Here the compact and dense nature of the film is evident. Fig. 1(c) is a cross-section of the film. This image shows the sapphire-YIG interface and regions of dense YIG speckled by regions of voids. To estimate the density of the film from this image we calculate the area of the void regions within a selected area. From this we estimate 4% void content, or equivalently 96% of full density. We also weighed and measured the bulk volume of a film. Taking this ratio results in a density of $(4.63 \pm 0.04)$ g/cm$^3$ or 90% of the theoretical density. The as-deposited film shown in panels (a)–(c) has an average film thickness and RMS roughness of 1.61 μm and 0.2 μm, respectively. The ratio of RMS roughness to thickness is 12%. This is close to the roughness-to-thickness ratio of about 10% we found in other AD YIG films produced in this system.

Fig. 2 shows SEM images of another film after a 1000 °C anneal as a comparison to the as-deposited film. Fig. 2(a) and (b) shows the top of the film at the same magnifications as the as-deposited film. A comparison between the images in Figs. 1 and 2 indicates that significant grain growth has occurred. The FIB cross-section shown in Fig. 2(c) shows that the film has reached full density with the exception of thermally induced cracking at the surface.

Fig. 3 shows a plot of the 2 theta-omega scan of a 1000 °C annealed film and an as-deposited YIG film stacked above the International Center for Diffraction Data (ICDD) 01-083-1027 card

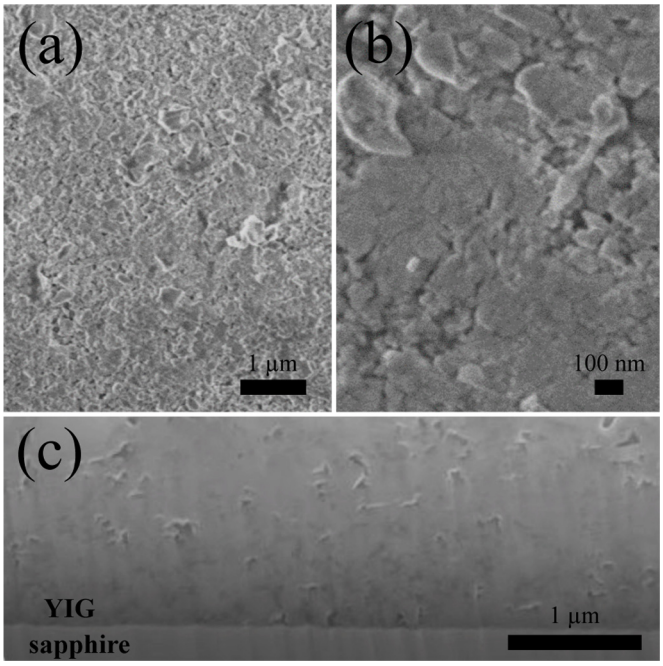


**Fig. 1.** SEM images of an as-deposited YIG film. Images (a) and (b) show the nano-structured and compact nature of the top surface of the film. Image (c) shows a cross-section of the film. The sapphire and YIG are labeled to clarify the interface. The dark regions are voids in the film. Based on images (b) and (c) it is evident that the film is dense throughout the film volume.